AGU PUBLICATIONS

Geophysical Research Letters

RESEARCH LETTER

10.1002/2014GL059426

Key Points:
- Observational evidence of Hadley cell widening and its regional structure

Supporting Information:
- Readme
- Figures S1–S4

Correspondence to:
S.-W. Son,
seokwooson@snu.ac.kr

Citation:
Choi, J., S.-W. Son, J. Lu, and S.-K. Min (2014), Further observational evidence of Hadley cell widening in the Southern Hemisphere, *Geophys. Res. Lett.*, *41*, doi:10.1002/2014GL059426.

Received 27 JAN 2014
Accepted 12 MAR 2014
Accepted article online 18 MAR 2014

Further observational evidence of Hadley cell widening in the Southern Hemisphere

Jung Choi[1], Seok-Woo Son[1], Jian Lu[2], and Seung-Ki Min[3]

[1]School of Earth and Environmental Sciences, Seoul National University, Seoul, South Korea, [2]Pacific Northwest National Laboratory, Richland, Washington, USA, [3]School of Environmental Science and Engineering, Pohang University of Science and Technology, Pohang, South Korea

Abstract Various observational and modeling studies have shown that the Hadley cell (HC) has widened during the past few decades. Here we present further observational evidence of the widening of the HC in the Southern Hemisphere by tracking the location of the subtropical ridge. A robust and significant poleward shift of the southern edge of the HC has been observed during the austral summer over the past three decades with a shift of 0.22° per decade between 1980 and 2012, primarily from the South Atlantic Ocean eastward to Australia. In other seasons, significant changes in the southern edge of the HC have not been observed, with a discernable regional trend having only occurred in limited regions. The comparison of these results with those derived from reanalysis data and possible causes for the summer HC expansion in the Southern Hemisphere are briefly discussed.

1. Introduction

The poleward edge of the Hadley cell (hereafter HC edge) plays a key role in determining the location of the subtropical dry zone, which is important not only for the hydrological cycle but also for the global energy budget of the Earth's climate system [*Seidel et al.*, 2008]. Various metrics have been suggested to identify the location of the HC edge that includes the use of measures of atmospheric circulation, satellite observations, and surface measurements. Although the resulting trends vary considerably depending on the metrics and data sets employed, most studies have shown an overall widening of the HC in the past (approximately 0.5–1.0° per decade widening in each hemisphere since 1979), as well as in future projections. However, the interhemispheric asymmetry and seasonality still remain unclear (see recent reviews by *Seidel et al*. [2008], *Davis and Rosenlof* [2012], and *Lucas et al*. [2014]).

The mass stream function (MSfn) is one of the most common metrics. Its zero-crossing latitude in the midtroposphere has been commonly used to identify the HC edge [*Hu and Fu*, 2007; *Lu et al*., 2007; *Min and Son*, 2013]. Tropopause-based methods [e.g., *Seidel and Randel*, 2007; *Davis and Rosenlof*, 2012; *Lucas et al*., 2012] and the location of subtropical jets [e.g., *Seidel et al*., 2008; *Allen et al*., 2012] have also been widely used. These metrics, however, have not been directly applied to observations because of the limited spatial coverage of the observational network, especially in the Southern Hemisphere (SH). To find observational evidence of changes in the HC edge, recent studies have also utilized satellite observations of outgoing long-wave radiation [*Chen et al*., 2002], total ozone concentrations [*Hudson et al*., 2006], global air temperatures [*Fu et al*., 2006], and cloudiness measurements [*Zhou et al*., 2011]. These metrics typically measure the difference between the tropical and subtropical upper tropospheric conditions, but they suffer from arbitrary thresholds in defining the HC edge. Meanwhile, surface measurements, such as precipitation minus evaporation [*Previdi and Liepert*, 2007], sea level pressure (SLP) [*Hu et al*., 2011, hereafter H11], and surface wind [*Staten et al*., 2012], have been utilized as well. Among these measurements, direct and global observations for extended time periods are only available for SLP.

With the purpose of expanding upon and updating the aforementioned studies, the present study provides further observational evidence of a widening of the HC in the SH through the detection of the poleward edge of the HC using SLP fields from reconstructed observation and reanalysis data sets. Specifically, the location of the subtropical ridge (i.e., the maximum SLP in the subtropics) is used to identify the HC edge. Unlike in previous studies, though, both the zonal mean and regional structures are quantified in this study.

2. Data and Methodology

The key data used in this study are near-real-time updates of the Hadley Centre's monthly mean SLP (HadSLP2r) [*Allan and Ansell*, 2006]. Only the last 54 years (1959–2012) of HadSLP2r are used to ensure a reliable analysis [*L'Heureux et al.*, 2013]. The results are compared with those derived from long-term reanalysis data sets, which include the European Centre for Medium-range Weather Forecasts' (ECMWF) 40 year reanalysis (ERA40), the Twentieth Century Reanalysis (20CR), the National Centers for Environmental Prediction (NCEP)-National Center for Atmospheric Research Reanalysis (NCEP1), and the Japanese 55 year Reanalysis (JRA55) data sets from December 1958 onward. For the postsatellite era, additional data sets are also considered, including the ECMWF Interim Reanalysis (ERAint), the Japanese 25 year Reanalysis (JRA25), the Modern Era Retrospective Analysis for Research and Applications (MERRA), the NCEP-Department of Energy Reanalysis (NCEP2), and the Climate Forecast System Reanalysis (CFSR) data sets from December 1979 onward. These data sets cover all reanalysis data currently available. To match the HadSLP2r, the SLP data from all reanalysis data sets were interpolated into a 5° × 5° grid before analysis. Although not shown, using a higher resolution (e.g., 2.5° × 2.5°) produced essentially the same results. Other fields of interest, such as meridional wind, are interpolated into a 2.5° × 2.5° grid at 17 pressure levels ranging from 1000 hPa to 10 hPa to reduce the uncertainty associated with different horizontal resolution among the data. Only monthly mean data is used, and statistical significance is tested by bootstrap method (see the supporting information in detail).

The poleward edge of the HC is identified by the location of the subtropical high [*Drosdowsky*, 2005; H11; *Timbal and Drosdowsky*, 2013] specifically defined by the location where $d\mathrm{SLP}/dy = 0$. The monthly SLP field is first averaged over seasons or years and then integrated in longitudes. Its meridional gradient is then computed using the fourth-order centered difference, and the zero-crossing latitude (i.e., the latitude where $d\mathrm{SLP}/dy = 0$) is determined by means of linear interpolation. This approach is different from H11 who detected HC edge by tracking maximum SLP using the cubic spline interpolation. In the case of the regional edge of the HC (more precisely, the local subtropical ridge), zonal integration is ignored and overall analysis is performed at each longitude (i.e., on the 5° longitude width).

The SLP-based HC edge is closely related to the canonical definition of the HC edge that is a zero-crossing latitude of MSfn in the midtroposphere. The steady state quasi-geostrophic zonal mean momentum budget can be considered as

$$-\frac{\partial\overline{[u^*v^*]}}{\partial y} + f\overline{[v]} - \frac{\overline{[u]}}{\tau} = 0 \tag{1}$$

where the brackets and asterisks denote the zonal mean and deviation from the zonal mean, respectively. The overbar indicates the monthly or seasonal mean. The last term on the left side of the equation denotes surface friction, which is parameterized as a linear damping with a timescale of τ. All of the other symbols used in equation (1) are standard in the atmospheric sciences.

In the free atmosphere, the dominant balance in equation (1) is between the first and second terms. Integrating equation (1) vertically from the top of the atmosphere to 500 hPa yields

$$\int_0^{500\mathrm{hPa}} \overline{[v]}\, dp = \int_0^{500\mathrm{hPa}} \frac{1}{f}\frac{\partial\overline{[u^*v^*]}}{\partial y}\, dp. \tag{2}$$

This indicates that the HC edge, if defined by the zero-crossing latitude of MSfn at 500 hPa that is proportional to the left side of equation (2), collocates with the latitude where the vertically integrated eddy momentum flux convergence in the *upper troposphere* changes sign. If the vertical integration is further extended to the surface, the main balance in equation (1) becomes

$$\overline{[u]}_{\mathrm{surface}} = -\int_0^{\mathrm{surface}} \tau \frac{\partial\overline{[u^*v^*]}}{\partial y}\, dp. \tag{3}$$

Here it is assumed that the meridional flow of mass in the upper level is completely canceled out by the return flow in the lower level. Given the fact that the zonal mean zonal wind at the surface changes signs where $d[\mathrm{SLP}]/dy = 0$, the HC edge defined by the subtropical ridge corresponds to the latitude where the vertically integrated eddy momentum flux convergence in the *whole troposphere* changes signs. As such, the MSfn-based HC edge is constrained by the eddy fluxes in the upper troposphere, while the SLP-based HC edge is more tightly constrained by the eddy fluxes in the whole troposphere.

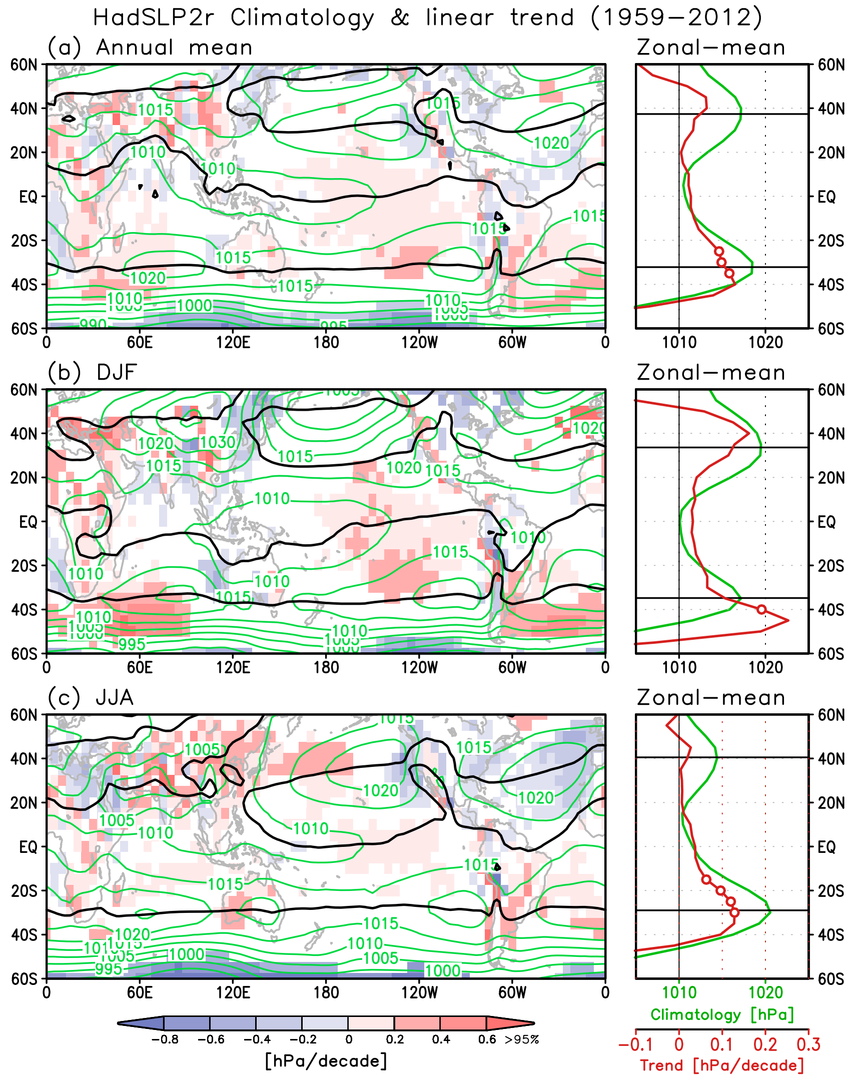

Figure 1. Spatial distribution and zonal mean of climatological SLP (green lines) over the period of 1959–2012 for the (a) annual mean, (b) austral summer, and (c) winter from HadSLP2r. Linear trends that are statistically significant at the 95% confidence level are shown by shading in Figures 1a–1c (left) and red-marked lines in Figures 1a–1c (right). Black lines denote the zero-crossing latitude of the meridional gradient of climatological SLP. A bootstrap method is used to test significance.

Equations (2) and (3) clearly suggest that the SLP-based HC edge is dynamically related to the MSfn-based HC edge through the eddy momentum fluxes. However, it is important to note that the SLP is modulated not only by large-scale atmospheric circulation but also by local thermodynamics. For example, differential heating between the land and ocean, which is not related to atmospheric circulation, can change the climatology and long-term trends of SLP [*Bayr and Dommenget*, 2013]. Therefore, climatology and temporal variability of the HC edge derived from the SLP field are not necessarily the same as those calculated from MSfn.

3. Results

Figure 1 presents the spatial distribution and zonal mean of the climatological SLP (green contour line) and their linear trends over the period 1959–2012 (shading in Figures 1a–1c (left) and the red line in Figures 1a–1c (right)) from HadSLP2r. The zero-crossing latitude of $d\mathrm{SLP}/dy$ is indicated by the black line. From these results, it can be seen that the subtropical ridge is well defined and zonally symmetric in the SH, whereas in the Northern Hemisphere (NH) it is highly asymmetric. More importantly, the subtropical ridge is not well defined over the

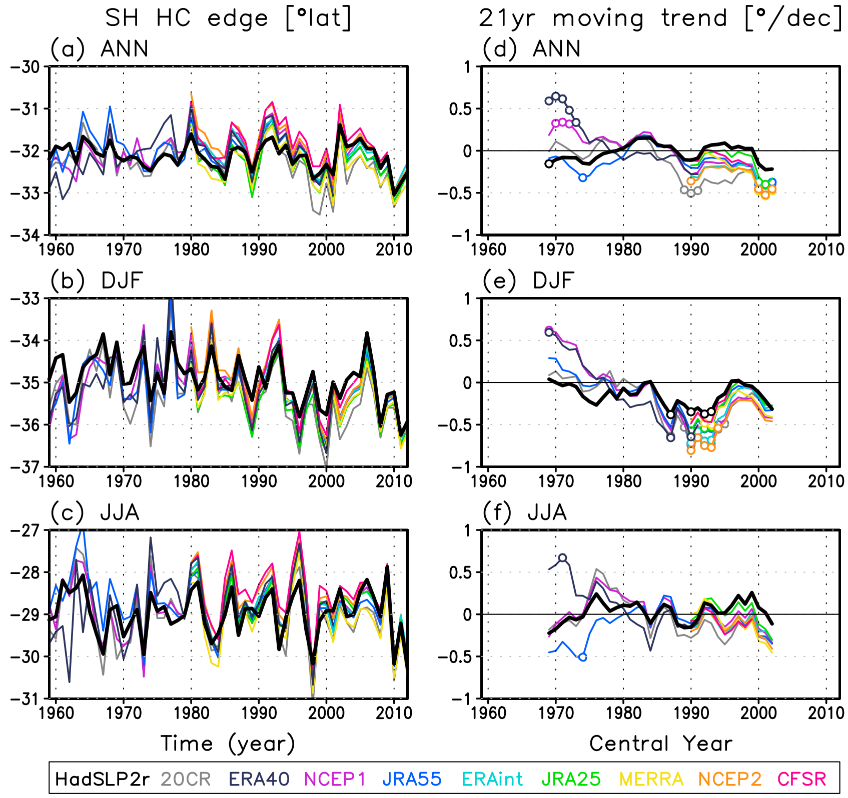

Figure 2. Time series and 21 year running linear trend of the SLP-based SH HC edge for the (a and d) annual mean, (b and e) austral summer, and (c and f) winter. Black and colored lines denote HadSLP2r and reanalysis data, respectively. Linear trends that are statistically significant at the 95% confidence level are shown by open circles in Figures 2d–2f. A bootstrap method is used to test significance.

Eurasian continent, presumably because of monsoon circulations and the region's complex topography. This suggests that the subtropical ridge may not be a practical metric for defining the local poleward edge of the HC in the NH.

It is also evident from Figure 1 that the SH SLP has increased significantly since 1959 especially around the subtropical ridge. This is most noticeable over the South Indian and Atlantic Oceans during the austral summer (December, January, and February (DJF), Figure 1b). On average, maximum zonal mean SLP trend is found on the poleward side of the climatological SH HC edge, indicating poleward shift of the HC edge during the last 54 years.

Figures 2a–2c present the time series of the SLP-based HC edge in the observation and reanalysis data. The HadSLP2r (black line) shows a climatological HC edge near 34.9°S in the austral summer and 29.0°S in the winter, which is indicative of seasonal migration of the HC edge. The results are consistent with the MSfn-based HC edge [e.g., *Nguyen et al*., 2013]. This strong seasonal cycle is to a large degree caused by the local edge over the South Pacific with a rather weak seasonality around the Indian Ocean and the South Atlantic (Figure 1 and Figure S1a in the supporting information). On top of the seasonal cycle, significant interannual to decadal variability exists both in the observation and reanalysis data (Figure S1b). Although the zonal mean HC edges derived from the reanalysis data vary among the data sets, they generally spread about the observation with a maximum bias of less than 2° during the postsatellite era.

Table 1 summarizes the linear trend of the HC edge from HadSLP2r and six selected reanalysis data sets. Statistically significant negative (poleward) trends are found during the austral summer (DJF) and autumn (March, April, and May (MAM)) over the period of 1959–2012, which is consistent with past widening of the HC observed from other metrics [H11; *Nguyen et al*., 2013]. These trends can primarily be observed during the last three decades of the period, with a change of −0.22°–−0.45° per decade in summer over the period of 1980–2012. Although a discernable autumn trend can also be seen during this time period, it was found to be

Table 1. Observed Linear Trend for the HC Edge in the SH Over the Period of 1959–2012, 1980–2012, and 1980–2000 for the Annual Mean (ANN), Austral Summer (DJF), Autumn (MAM), Winter (JJA), and Spring (SON) From (top) HadSLP2r and (bottom) Six Selected Reanalyses[a]

Period	ANN	DJF	MAM	JJA	SON
1959–2012	−0.05	−0.15[b]	−0.11[b]	−0.03	0.01
1980–2012	−0.08	−0.22[b]	−0.16	−0.06	−0.07
1980–2000	−0.11	−0.35[b]	−0.22	−0.15	0.03
1980–2012	−0.14 to 0.30[b]	−0.26[b] to −0.45[b]	−0.25 to −0.41[b]	−0.11 to −0.23	−0.12 to −0.27[b]
1980–2000	−0.11 to −0.36[b]	−0.46 to −0.81[b]	−0.24 to −0.61	−0.003 to −0.20	−0.01 to −0.24

[a]Negative trends indicate a poleward widening of the HC edge in the SH. Units are (latitude/decade).
[b]Linear trends that are statistical significant at the 95% confidence level by a bootstrap method.

statistically insignificant. If only the last two decades of the twentieth century are considered, an even stronger trend of −0.35°–−0.81° per decade can be observed in summer. This indicates that the long-term trend of the HC edge is not necessarily linear as hinted at by Figures 2a–2c. To identify the period when the trend is strong and significant, 21 year running linear trends have been computed as shown in Figures 2d–2f. In Figures 2d–2f, the years along the *x* axis denote the central year of the time period of the trend; for example, 1990 indicates the trend computed from 1980 to 2000. The HC edge derived from HadSLP2r shows statistically significant negative trends during the austral summer in the late twentieth century. Trends of significance also occur at the similar periods in most of the reanalysis data (Figure 2e; see also H11), assigning confidence to both the amplitude and the timing of the HC expansion of the SH summer. This contrasts with the winter trend, which is insignificant during almost all time periods (Figure 2f). Although significant trends can also be seen in the annual mean SH HC edge around 1990 and 2000 in some reanalysis data (Figure 2d), these trends are not robust across the data sets.

Figure 3 presents the linear trends of the SLP-based HC edge and their relationship to the MSfn-based HC trends over the period of 1980–2012 when the data is mostly reliable (see also Figure S2 for the time period of

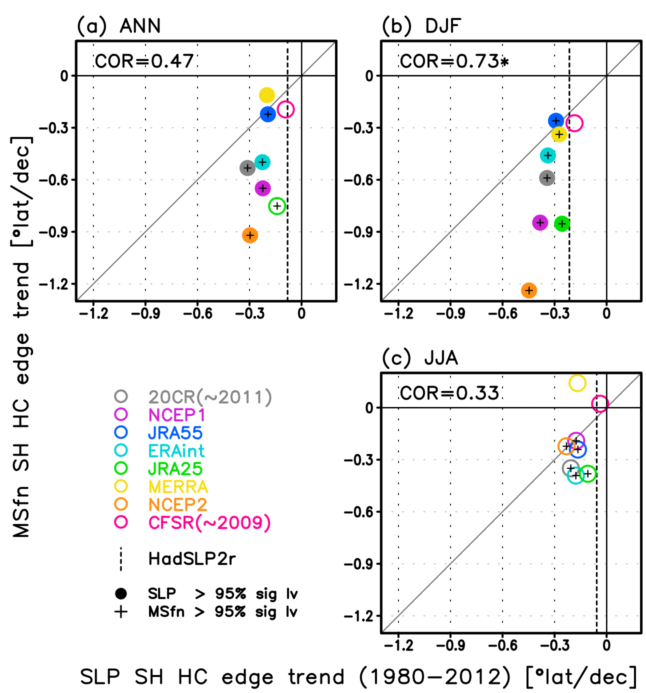

Figure 3. Scatterplots of linear trends for the SLP-based and MSfn-based SH HC edge over the period of 1980–2012 for the (a) annual mean, (b) austral summer, and (c) winter. The black dashed vertical line indicates the linear trend of HadSLP2r. The circle with a filled circle (cross mark) represents the significant SLP-based (MSfn-based) trend at the 95% confidence level. Correlations of SLP-based indices against the MSfn-based indices are denoted in each figure. Asterisks correspond to correlations that are statistically significant at the 95% confidence level.

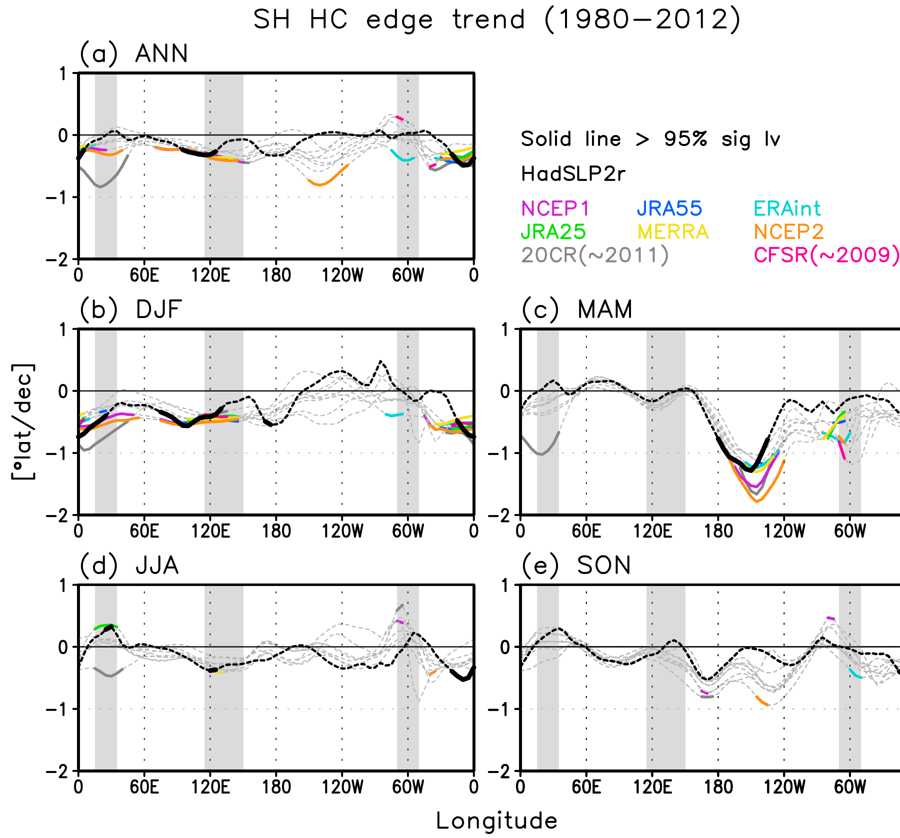

Figure 4. Longitudinal distributions of linear trends of the SLP-based regional edge of the HC in the SH over the period of 1980–2012 for the (a) annual mean, (b) austral summer, (c) autumn, (d) winter, and (e) spring. Linear trends that are statistically significant at the 95% confidence level are shown by a colored solid line. Gray-shaded regions denote the longitude where land exists between 40°S and 25°S. A bootstrap method is used to test significance.

1980–2000). The observed trend is indicated by the vertical dashed line, and each reanalysis data is denoted by a circle, where the filled circles indicate significant SLP-based trends, and cross marks indicate significant MSfn-based trends. It can readily be seen that the magnitude of HC trend is generally larger in the reanalysis data compared to HadSLP2r in both the summer and winter seasons (see also H11). It can also be seen that as expected from equations (2) and (3), the SLP-based HC edge trends are positively correlated with the MSfn-based ones in the reanalysis data in all seasons. The correlation is particularly significant in summer. However, in winter (when eddy activities are relatively weak to the thermally forced wind), the correlation is rather weak and statistically insignificant. This indicates that the SLP-based HC trends are affected not only by eddy fluxes but also by other physical processes such as local thermodynamics. It is worth noting that the interdata spread of the SLP-based HC edge trends is much narrower than that of the MSfn-based ones, as can be seen in Figure 3. This is presumably because the SLP-based metrics are more tightly constrained by the eddy fluxes as discussed in section 2 and also because the SLP reanalysis assimilated surface observations (e.g., the surface temperature and in situ SLP) while meridional wind fields are not well constrained by observations. Furthermore, it can be seen that on interannual timescales, the SLP-based HC edge is well correlated with the MSfn-based one in all seasons (Figure S3).

Are the long-term trends shown in Table 1 and Figure 3 homogeneous within longitudes? Figure 4 presents the linear trend of the regional edge of the HC over the period of 1980–2012 (see Figure S4 for trends over the years of 1980–2000). To eliminate the effects of local circulation and topography, a 30° longitudinal-moving average is applied to the SLP field before the analysis. It can be seen that the regional edge of the HC trends is not zonally symmetric. Even in summer when the poleward shift of the HC edge is strongest, statistically significant trends are found only from the South Atlantic Ocean eastward to Australia where interannual variability is relatively small (Figure S1b). This suggests that the expansion of the HC in the SH may have different implications for different regions [*Cai et al*., 2012]. In other seasons, statistically significant trends are sporadically found in relatively small regions, such as over the South Atlantic in winter (June, July, and August (JJA)) and spring (September, October, and November (SON)) and over the central South Pacific in autumn (MAM). This result is consistent with a weak zonal mean HC trend in these seasons. Nevertheless, the qualitative agreement between the reanalyses and the HadSLP2r data is encouraging; the cross validation between them gives us some confidence in some of the significant regional features of expansion.

It is noteworthy that a strong but statistically insignificant HC trend in autumn (Table 1) is caused by a local trend over the South Pacific Ocean. This local trend is likely caused by wave response to equatorial sea surface temperatures (SST) instead of a large-scale zonal mean circulation change [*Mullan*, 1998]. Additionally, recent studies have shown that changes in SST, such as long-term trends of El Nino–Southern Oscillation and Pacific Decadal Oscillation, may have also influenced the HC trend in MAM [H11; *Grassi et al*., 2012]. In fact, the interannual variability of the HC edge is also largest over this region (Figure S1b), and linear trends are sensitive to the choice of the analysis time period (Figure S4c).

4. Summary and Discussion

This study presents observational evidence of a widening of the Hadley cell (HC) and its regional structure in the Southern Hemisphere (SH) by tracking the location of the subtropical ridge in the reconstructed sea level pressure (SLP) field, which is one of the most reliable observations during the last five decades. It has been found that at least in the SH, the SLP-based HC edge is a reliable metric for identifying the temporal variability of the HC edge across timescales. A significant correlation was also observed in linear trends during the summer between the SLP-based HC edge and the canonical stream function-based one. While these results suggest that the SLP-based HC edge is a useful metric for quantifying the SH zonal mean circulation change, it is important to note that the SLP-based metric is applicable to observations and can be extended to detect regional changes.

The HC edge has shown a robust and statistically significant poleward shift during the austral summer (DJF) during the past three decades, with a significant poleward shift of 0.22°–0.45° per decade having been observed during the period of 1980–2012. Regional analyses show that this shift has primarily occurred around from the South Atlantic Ocean eastward to Australia. In other seasons, the trends are significant only in limited regions and largely inhomogeneous across longitudes, showing little relation to zonal mean circulation changes. These findings support the notion of *Cai et al*. [2012] regarding the zonally asymmetric circulation features associated with the HC expansion. Although the results from zonal mean and regional analyses are qualitatively consistent among the data sets, the HadSLP2r showed a generally smaller trend than the values from reanalysis. This might result from sampling errors particularly in high southern latitudes in both HadSLP2r and reanalysis data [*Allan and Ansell*, 2006].

What drives a poleward shift of the HC edge during the austral summer? Numerous studies have been conducted recently to investigate the possible causes of the SH HC expansion since the late 1970s (see recent review by *Lucas et al*. [2014]). A consensus seems to have emerged that both the effects of increasing greenhouse gases and decreasing stratospheric ozone concentrations have contributed to the expansion trend [*McLandress et al*., 2011; *Polvani et al*., 2011; *Min and Son*, 2013]. In late 1990s, stratospheric ozone concentration started to plateau due to the implementation of the Montreal Protocol [*Eyring et al*., 2013]. As ozone concentrations are projected to increase in the 21st century, the impact of ozone on SH circulation is expected to offset that of increases in greenhouse gases [*Son et al*., 2010; *McLandress et al*., 2011]. The tapering of the expansion trend in the summer HC at the end of the twentieth century (as shown in Figure 2e) might not be just a coincidence.

Acknowledgments
This study was supported by the Basic Science Research Program through the National Research Foundation of Korea (NRF) funded by the Ministry of Education (2013R1A1A1006530 and 2013R1A6A3A01020749). J.L. was supported by the Office of Science of the U.S. DOE as part of the Regional and Global Climate Modeling and Integrated Assessment Research programs. The PNNL is operated for DOE by Battelle Memorial Institute under contract DE-AC05-76RL01830.

The Editor thanks two anonymous reviewers for assistance evaluating this manuscript.

References

Allan, R., and T. Ansell (2006), A new globally complete monthly historical gridded mean sea level pressure dataset (HadSLP2): 1850–2004, *J. Clim.*, *19*, 5816–5842.

Allen, R. J., S. C. Sherwood, J. R. Norris, and C. S. Zender (2012), Recent Northern Hemisphere tropical expansion primarily driven by black carbon and tropospheric ozone, *Nature*, *485*, 350–354.

Bayr, T., and D. Dommenget (2013), The tropospheric land-sea warming contrast as the driver of tropical sea level pressure changes, *J. Clim.*, *26*, 1387–1402.

Cai, W., T. Cowan, and M. Thatcher (2012), Rainfall reductions over Southern Hemisphere semi-arid regions: The role of subtropical dry zone expansion, *Sci. Rep.*, *2*, doi:10.1038/srep00702.

Chen, J., B. E. Carlson, and A. D. Del Genio (2002), Evidence for strengthening of the tropical general circulation in the 1990s, *Science*, *295*, 838–841.

Davis, S. M., and K. H. Rosenlof (2012), A multi diagnostic intercomparison of tropical-width time series using reanalyses and satellite observations, *J. Clim.*, *25*, 1061–1077.

Drosdowsky, W. (2005), The latitude of the subtropical ridge over eastern Australia: The L index revisited, *Int. J. Climatol.*, *25*, 1291–1299, doi:10.1002/joc.1196.

Eyring, V., et al. (2013), Long-term ozone changes and associated climate impacts in CMIP5 simulations, *J. Geophys. Res. Atmos.*, *118*, 5029–5060, doi:10.1002/jgrd.50316.

Fu, Q., C. M. Johanson, J. M. Wallace, and T. Reichler (2006), Enhanced mid-latitude tropospheric warming in satellite measurements, *Science*, *312*, 1179, doi:10.1126/cience.1125566.

Grassi, B., G. Redaelli, P. O. Canziani, and G. Visconti (2012), Effects of the PDO phase on the tropical belt width, *J. Clim.*, *25*, 3282–3290.

Hu, Y., and Q. Fu (2007), Observed poleward expansion of the Hadley circulation since 1979, *Atmos. Chem. Phys.*, *7*, 5229–5236.

Hu, Y., C. Zhou, and J. Liu (2011), Observational evidence for the poleward expansion of the Hadley circulation, *Adv. Atmos. Sci.*, *28*, 33–44.

Hudson, R. D., M. F. Andrade, M. B. Follette, and A. D. Frolov (2006), The total ozone field separated into meteorological regimens—Part II: Northern hemisphere mid-latitude total ozone trends, *Atmos. Chem. Phys.*, *6*, 5183–5191.

L'Heureux, M. L., S. Lee, and B. Lyon (2013), Recent multidecadal strengthening of the Walker circulation across the tropical Pacific, *Nat. Clim. Change*, *3*, 571–576.

Lu, J., G. A. Vecchi, and T. Reichler (2007), Expansion of the Hadley cell under global warming, *Geophys. Res. Lett.*, *34*, L06805, doi:10.1029/2006GL028443.

Lucas, C., H. Nguyen, and B. Timbal (2012), An observational analysis of Southern Hemisphere tropical expansion. *J. Geophys. Res.*, *117*, D17112, doi:10.1029/2011JD01733.

Lucas, C., B. Timbal, and H. Nguyen (2014), The expanding tropics: A critical assessment of the observational and modeling studies, *WIREs Clim. Change*, *5*, 89–112, doi:10.1002/wcc.251.

McLandress, C., T. G. Shepherd, J. F. Scinocca, D. A. Plummer, M. Sigmond, A. I. Jonsson, and M. C. Reader (2011), Separating the dynamical effects of climate change and ozone depletion. Part II: Southern Hemisphere troposphere, *J. Clim.*, *24*, 1850–1868.

Min, S.-K., and S.-W. Son (2013), Multi-model attribution of the Southern Hemisphere Hadley cell widening: Major role of ozone depletion, *J. Geophys. Res. Atmos.*, *118*, 3007–3015, doi:10.1002/jgrd.50232.

Mullan, A. B. (1998), Southern Hemisphere sea-surface temperatures and their contemporary and lag association with New Zealand temperature and precipitation, *Int. J. Climatol.*, *18*, 817–840.

Nguyen, H., A. Evans, C. Lucas, I. Smith, and B. Timbal (2013), The Hadley circulation in reanalyses: Climatology, variability and expansion, *J. Clim.*, *26*, 3357–3376, doi:10.1175/JCLI-D-12-00224.

Polvani, L. M., D. W. Waugh, G. J. P. Correa, and S.-W. Son (2011), Stratospheric ozone depletion: The main driver of twentieth-century atmospheric circulation changes in the Southern Hemisphere, *J. Clim.*, *24*, 795–812.

Previdi, M., and B. G. Liepert (2007), Annual modes and Hadley cell expansion under global warming, *Geophys. Res. Lett.*, *34*, L22701, doi:10.1029/2007GL031243.

Seidel, D. J., and W. J. Randel (2007), Recent widening of the tropical belt: Evidence from tropopause observations, *J. Geophys. Res.*, *112*, D20113, doi:10.1029/2007JD008861.

Seidel, D. J., F. Qiang, W. J. Randel, and T. J. Reichler (2008), Widening of the tropical belt in a changing climate, *Nat. Geosci.*, *1*, 21–24.

Son, S.-W., et al. (2010), Impact of stratospheric ozone on Southern Hemisphere circulation change: A multimodel assessment, *J. Geophys. Res.*, *115*, D00M07, doi:10.1029/2010JD014271.

Staten, P. W., J. J. Rutz, T. Reichler, and J. Lu (2012), Breaking down the tropospheric circulation response by forcing, *Clim. Dyn.*, *39*, 2361–2375.

Timbal, B., and W. Drosdowsky (2013), The relationship between the decline of southeastern Australian rainfall and the strengthening of the subtropical ridge, *Int. J. Climatol.*, *33*, 1021–1034, doi:10.1002/joc.3492.

Zhou, Y. P., K.-M. Xu, Y. C. Sud, and A. K. Betts (2011), Recent trends of the tropical hydrological cycle inferred from Global Precipitation Climatology Project and International Satellite Cloud Climatology Project data, *J. Geophys. Res.*, *116*, D09101, doi:10.1029/2010JD01597.